A compact data structure for high dimensional Coxeter-Freudenthal-Kuhn triangulations

Jean-Daniel Boissonnat, Siargey Kachanovich, Mathijs Wintraecken

A compact data structure for high dimensional Coxeter-Freudenthal-Kuhn triangulations

Jean-Daniel Boissonnat
Université Côte d'Azur, Inria
[Sophia-Antipolis, France]
jean-daniel.boissonnat@inria.fr

Siargey Kachanovich
Université Côte d'Azur, Inria
[Sophia-Antipolis, France]
siargey.kachanovich@inria.fr

Mathijs Wintraecken
IST Austria
[Klosterneuburg, Austria]
m.h.m.j.wintraecken@gmail.com

—— **Abstract** ——

We consider a family of highly regular triangulations of $\mathbb{R}^d$ that can be stored and queried efficiently in high dimensions. This family consists of Freudenthal-Kuhn triangulations and their images through affine mappings, among which are the celebrated Coxeter triangulations of type $\tilde{A}_d$. Those triangulations have major advantages over grids in applications in high dimensions like interpolation of functions and manifold sampling and meshing. We introduce an elegant and very compact data structure to implicitly store the full facial structure of such triangulations. This data structure allows to locate a point and to retrieve the faces or the cofaces of a simplex of any dimension in an output sensitive way. The data structure has been implemented and experimental results are presented.

2012 ACM Subject Classification Theory of computation → Computational geometry

Keywords and phrases Spatial subdivisions, High dimensional computational geometry, Coxeter triangulation, Kuhn triangulation, permutahedrons

1 Introduction

Subdivisions of Euclidean space are a major tool to efficiently answer geometric queries, compute approximation of shapes or solve optimization problems. Among the most widely used subdivision schemes are grids and triangulations. Both are subject to the curse of dimensionality and their combinatorial complexity depends exponentially on the dimension of the space. Triangulations are most flexible since their vertex set can be any set of points. Differently, uniform grids depend only on the space but not on a given data set. The rigidity
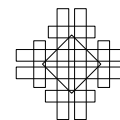
of the grid structure has a major advantage: the grid, although of exponential size, need not be represented explicitly and basic operations like locating a point or computing faces or cofaces of a given cell in the grid can be done without storing an explicit representation of the grid. In fact, the representation can be entirely implicit. This is clearly impossible with general triangulations with arbitrary vertex sets.

The question of designing efficient data structure for triangulations and more general simplicial complexes led to interesting developments recently. On one hand, one can take advantage of the fact that special types of simplicial complexes allow compact representations. Most notably, flag complexes (including the celebrated Vietoris-Rips complex) can be represented by their 1-skeleton (or graph) and higher dimensional faces can be retrieved by computing the cliques of the graph. One can also represent a simplicial complex by its blockers, i.e. the simplices that do not belong to the complex but whose facets do [3].

On a different front, data structures have been proposed to efficiently store general simplicial complexes such as the simplex tree [7] that uses a trie to store the faces of all dimensions, or the Simplex Array List [6] that represents only the maximal faces, which allows an exponential saving in storage since a simplex has exponential complexity. Nevertheless, due to their generality and the fact that the represented complexes don't have any prespecified symmetry, the data structures cannot compete with grids in terms of size and efficiency.

This paper explores middle ground and considers a special class of triangulations of $\mathbb{R}^d$ that have a high regularity. We propose a data structure for such triangulations that can be as compact as for grids.

The class of triangulations we consider has different origins and names. The two foundational works are due to Coxeter [14] and Freudenthal [18]. Coxeter triangulations derive from geometric group theory, in particular affine Weyl groups, while Freudenthal triangulations (also called Kuhn triangulations) are combinatorial in nature. Nevertheless, both triangulations are the same up to a linear transformation, as remarked in [15] and fully proved in this paper. This allows us to combine the nice geometric properties of Coxeter triangulations of type $\tilde{A}_d$ with the simple combinatorial definitions of the Freudenthal-Kuhn triangulation, and its connection to permutahedra. Coxeter triangulations of type $\tilde{A}_d$ are geometrically attractive because each simplex is very well shaped (large volume compared to longest edge length), and all d-simplices are identical up to reflections.

Although these triangulations do not depend on a given data set, they proved to be very useful in to interpolate multivariate multivalued functions or to mesh geometric shapes embedded in high dimensional spaces. Freudenthal-Kuhn triangulations have been known in Applied Mathematics [1, 16, 25], and Coxeter triangulations have been used by Dobkin et al. [15] to trace curves in high dimensions and are good candidates to trace manifolds of any codimension [21, 4]. They have also been used in the context of Topological Data Analysis [12].

In Section 2, we study these triangulations. This section recalls and extends to arbitrary dimensions several results that were disseminated in many different places which are sometimes difficult to access (see among others [18, 25, 16, 20, 27, 23, 15]).

Based on these results, we introduce in Section 3 a very compact data structure that implicitly stores the full facial structure of such triangulations. The data structure allows to locate a point in the triangulation and to retrieve the faces or the cofaces of a simplex of any dimension in an output sensitive way.

The Data Structure has been implemented and fully tested. Section 4 reports on experimental results and demonstrates that the data structure is highly practical and can handle triangulations of high dimensional spaces. Using our data structure will allow to

extend the applicability of the methods based on such triangulations and to significantly improve their performance. It appears to be especially useful to trace low dimensional manifolds embedded in high dimensional spaces as encountered in statistics, dynamical systems, econometrics, or mechanics [10, 25, 22].

2 Coxeter-Freudhental-Kuhn triangulations

Freudenthal-Kuhn triangulations are combinatorial structures that come from a specific triangulation of the d-cube. Their connections to permutahedra is at the heart of our data structure. Coxeter triangulations, we introduce in Section 2.3, have a different flavour and come with very nice geometric properties. Since both types of triangulations are the same up to an affine transformation, as first noted by Dobkin et al [15], they have the same combinatorial structure and our data structure will be able to handle both of them.

Although most ideas in this section were known previously, we give full proofs of the results that were not explicitly mentioned or not proved in full generality in the literature.

2.1 Permutahedra

We write $[i] = \{1, \ldots, i\}$, and $[i, j] = \{i, \ldots, j\}$.

▶ **Definition 1** (Permutahedron)**.** *A d-permutahedron is a d-dimensional polytope, which is the convex hull $\mathcal{P}$ of all points in $\mathbb{R}^{d+1}$, the coordinates of which are permutations of $[d + 1]$. Formally, this convex hull can be written as:*

$$\mathcal{P} = \mathrm{conv}\{(\sigma(1), \ldots, \sigma(d+1)) \in \mathbb{R}^{d+1} \mid \sigma \in \mathfrak{S}_{d+1}\},$$

where $\mathfrak{S}_{d+1}$ denotes the set of permutations of $[d + 1]$.

$\mathcal{P}$ is at most d-dimensional since all its vertices lie on the hyperplane of equation

$$\sum_{i=1}^{d+1} x^i = \frac{d(d+1)}{2}.$$

Moreover, it can be shown that there are $d + 1$ affinely independent vertices in $\mathcal{P}$, proving that $\mathcal{P}$ is exactly d-dimensional (see for example [20, Lemma 3.4]). The facial structure of $\mathcal{P}$ is best described in terms of ordered partitions [27]. Refer to Figure 1.

▶ **Definition 2** (Ordered partition)**.** *Let T be a finite non-empty set, $|T|$ its cardinality, and $l \leq |T|$ a positive integer. An* ordered partition *of T in l parts is an ordered collection of l subsets $\omega = (\omega_1, \ldots, \omega_l)$, such that $\omega_i \subseteq T$, and $\{\omega_1, \ldots, \omega_l\}$ is a partition of T. The ω_i are called the* parts*. We write $OP_l[d]$ for the set of ordered partitions of $[d]$ with l parts, and just $OP[d]$ for the set of all ordered partitions of $[d]$.*

▶ **Definition 3** (Refinement)**.** *Let ω, and ϖ be two ordered partitions of $[d + 1]$ in l, and p parts respectively, with $1 \leq l \leq p \leq d + 1$. We say that ϖ is a* refinement *of ω if there exist positive integers $a_1, \ldots, a_l$, such that*

- $(\varpi_1, \ldots, \varpi_{a_1})$ *is an ordered partition of ω_1 in a_1 parts,*
- $(\varpi_{a_1+1}, \ldots, \varpi_{a_1+a_2})$ *is an ordered partition of ω_2 in a_2 parts,*
- $\ldots,$
- $(\varpi_{a_1+\ldots+a_{l-1}+1}, \ldots, \varpi_{a_1+\ldots+a_l})$ *is an ordered partition of ω_l in a_l parts.*

We recall Theorem 3.6 of [20]:

$$\{2\}, \{1\}, \{3\}$$

$\{2\}, \{1, 3\}$ $\{1, 2\}, \{3\}$

$$\{2\}, \{3\}, \{1\} \qquad\qquad \{1\}, \{2\}, \{3\}$$

$\{2, 3\}, \{1\}$ $\{1, 2, 3\}$ $\{1\}, \{2, 3\}$

$$\{3\}, \{2\}, \{1\} \qquad\qquad \{1\}, \{3\}, \{2\}$$

$\{3\}, \{1, 2\}$ $\{1, 3\}, \{2\}$

$$\{3\}, \{1\}, \{2\}$$
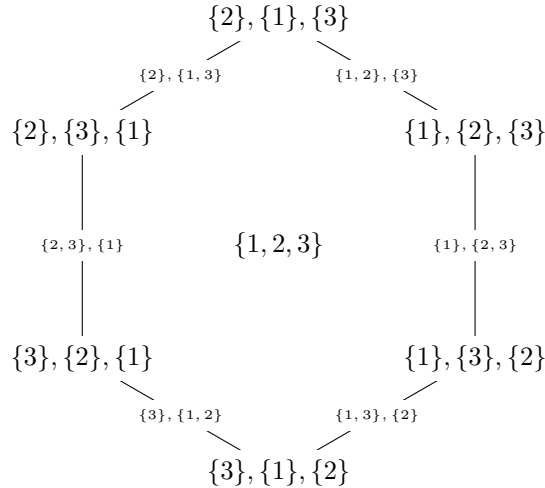
<p>91</p> ▮ **Figure 1** The 2-permutahedron and the ordered partitions associated to its faces.

<p>105</p> ▶ **Lemma 4** (Facial structure of the permutahedron). *The faces of a d-permutahedron are in*
<p>106</p> *bijection with the ordered partitions of $[d+1]$. More precisely, the i-faces of $\mathcal{P}$ correspond to*
<p>107</p> *ordered partitions of $[d+1]$ into $l = d+1-i$ parts $(\omega_1, \ldots, \omega_l)$. If σ, and τ are two faces of*
<p>108</p> *a d-permutahedron, σ is a subface of τ (denoted $\sigma \subseteq \tau$) if and only if the ordered partition*
<p>109</p> *associated to σ is a refinement of the ordered partition associated to τ.*

<p>110</p> We also need the following result from [20, Corollary 3.15], and [23, Theorem 3].

<p>111</p> ▶ **Corollary 5.** *The number of $(d-i)$-dimensional faces in a d-permutahedron is $(i+1)!\,S(d+$*
<p>112</p> *$1, i+1)$, where $S(\cdot, \cdot)$ is the Stirling number of the second kind. It is bounded by $2^{2(d+1)\log(i+1)}$.*

<p>113</p> The following three corollaries seem to be new.

<p>114</p> ▶ **Corollary 6.** *The number $p_{0,i}$ of vertices of a i-face of a d-permutahedron is at most $(i+1)!$,*
<p>115</p> *and at least $2^{\min(i,d-i)}$.*

<p>116</p> The proof of Corollary 6 is based on:

<p>117</p> ▶ **Lemma 7** (Lemma 3.11 of [20]). *The face of a permutahedron corresponding to an ordered*
<p>118</p> *partition $\omega = (\omega_1, \ldots, \omega_{l+1})$ is combinatorially*

<p>119</p> $$\mathcal{P}(|\omega_1|) \times \cdots \times \mathcal{P}(|\omega_{l+1}|),$$

<p>120</p> *where $|\omega_p|$ denotes the length of the p-th part of the ordered partition, and $\mathcal{P}(n)$ the permuta-*
<p>121</p> *hedron of dimension $n-1$.*

<p>122</p> **Proof of Corollary 6.** Write $l = d - i$. Since the number of vertices of the product of two
<p>123</p> polytopes is the product of the vertices, and a $(n-1)$-dimensional permutadedron has $n!$
<p>124</p> vertices, we see that the total number of vertices of a i-face of a d-dimensional permutahedron
<p>125</p> corresponding to an ordered partition $\omega = (\omega_1, \ldots, \omega_{l+1})$ is

<p>126</p> $$\prod_{p=1}^{l+1} (|\omega_p|!).$$

Let $1 \le j < k \le d$ be integers such that $j + k = d + 1$. By definition $j!k! < (j-1)!(k+1)!$, and thus $j!k! \le 1!d!$. Generalizing this, we see that the product of the $|\omega_p|!$ is maximal when all parts are singletons except the biggest part which has $d + 1 - l$ elements. Therefore

$$\prod_{p=1}^{l+1} (|\omega_p|!) \le (d - l + 1)!.$$

Using the inverse argument, the lower bound is obtained when each part in the ordered partition are as small as possible that is all parts have almost equal size. In this case, $|\omega_p| \ge \lfloor \frac{d+1}{l+1} \rfloor$, so that

$$\prod_{p=1}^{l+1} (|\omega_p|!) \ge \left(\left\lfloor \frac{d+1}{l+1} \right\rfloor ! \right)^{l+1}$$

More accurately, let r' be the remainder of $d + 1$ after division by $l + 1$, that is $r' = d + 1 \mod l + 1$ then:

$$\prod_{p=1}^{l+1} (|\omega_p|!) \ge \left(\left\lfloor \frac{d+1}{l+1} \right\rfloor ! \right)^{l-r'+1} \left(\left(\left\lfloor \frac{d+1}{l+1} \right\rfloor + 1 \right) ! \right)^{r'}$$

We now distinguish two cases:

- If $\lfloor \frac{d+1}{l+1} \rfloor \ge 2$, and thus $\frac{d+1}{2} \ge l + 1$, then we see that

$$\prod_{p=1}^{l+1} (|\omega_p|!) \ge 2^{l+1}.$$

- If $\lfloor \frac{d+1}{l+1} \rfloor = 1$, we have that $\frac{d+1}{2} < l + 1 \le d + 1$, and thus $r' = d + 1 \mod l + 1 = d - l$. Hence,

$$\prod_{p=1}^{l+1} (|\omega_p|!) \ge 2^{d-l}.$$

Because $l + 1 = d - l$, or $2l + 1 = d$ is precisely the point where you go from the first to the second case we see that

$$\prod_{p=1}^{l+1} (|\omega_p|!) \ge 2^{\min\{l+1, d-l\}}$$

◀

▶ **Corollary 8.** *The number of facets of an i-face σ of a d-permutahedron is at most 2^{i+1}.*

Proof. Write $l = d - i$. We first recall a set of $d > 2$ objects can be subdivided in two non-empty ordered subsets A and B in $2^d - 2$ ways. This is not hard to see. Because we pick for each element if it will be put in A or B there are 2^d possibilities. Excluding that A or B is empty gives $2^d - 2$. Let $\omega = (\omega_1, \dots, \omega_l)$ again be an ordered partition. To find a refinement of ω in $l + 1$ parts, we need to first pick a $1 \le p \le l$, such that $|\omega_p| > 1$, and then we need to break ω_p up into two (ordered) parts, for which there are $2^{|\omega_p|} - 2$ possibilities as we have seen above. This means that if $I = \{p \mid 1 \le p \le l, |\omega_p| > 1\}$, the number of refinements is

$$\sum_{p \in I} 2^{|\omega_p|} - 2.$$

Let now $1 \leq s < t \leq d$ be integers such that $s + t = d + 1$. Then $2^s + 2^t < 2^{s-1} + 2^{t+1}$. Generalizing this, we see that the sum of the $2^{|\omega_p|} - 2$ is maximal when all $|\omega_p| = 1$ except the biggest part which has $d - l + 1 = i + 1$ elements. ◄

▶ **Corollary 9.** *Let $p_{i,j}$ denote the number of i-faces of a j-face of the d-permutahedron. We have*

$$p_{i,j} \leq \frac{1}{2^{\min(i,d-i)}} \binom{j}{i} (j+1)!$$

Corollary 9 generalizes the previous two corollaries. For $i = 0$, the bound in Corollary 9 is the same as the upper bound in Corollary 6. For $i = j - 1$, the bound is comparable but weaker than the bound in Corollary 8.

Proof of Corollary 9. Let σ be a j-face of the d-permutahedron. Write $F_{i,\sigma}$ for the set of i-faces of σ, and c_v for the number of i-cofaces of a vertex v of σ, i.e. the number of simplices of $F_{i,\sigma}$ that contain v. For $\tau \in F_{i,\sigma}$, we write p_τ for the number of vertices of τ. By double counting the incidences between vertices, and i-faces inside σ, we have

$$\sum_{\tau \in F_{i,\sigma}} p_\tau = \sum_{v \in F_{0,\sigma}} c_v.$$

Now observe that the d-permutahedron is a simple polytope (this follows from the fact that its dual is simplicial since it is a star in the FK-triangulation). The faces of simple polytopes are also simple polytopes which implies that the vertices of a j-face are incident to $\binom{j}{i}$ faces of dimension i [8, Lemma 7.1.14]. Moreover, $|F_{0,\sigma}| \leq (j+1)!$ by Corollary 6. Hence

$$\sum_{v \in F_{0,\sigma}} c_v = \binom{j}{i} |F_{0,\sigma}| \leq \binom{j}{i} (j+1)!.$$

In addition, by Corollary 6, we have

$$\sum_{\tau \in F_{i,\sigma}} p_\tau \geq 2^{\min(i,d-i)} |F_{i,\sigma}|$$

The inequality follows since σ is any j-face of the d-permutahedron. ◄

2.2 Freudenthal-Kuhn triangulation

The Freudenthal-Kuhn (FK for short) triangulation is obtained from the d-grid, i.e. the unit cubical tessellation of $\mathbb{R}^d$ that consists of copies of the unit d-cube along the integer lattice $\mathbb{Z}^d$. By triangulating each d-cube in the grid in an appropriate way to be described now, we obtain the FK-triangulation of $\mathbb{R}^d$. The results and definitions below were known to Freudenthal [18], Todd [25], or Eaves [16], mainly for top dimensional simplices and in different guises. We combine these results and extend to simplices of arbitrary (co)dimension, where necessary.

▶ **Definition 10.** *Let $x \in \mathbb{R}^d$, and write $z^i = x^i - \lfloor x^i \rfloor$. We denote by $e_1, \ldots, e_d$ the basis vectors and introduce, for reasons that will be clear later, the extra vector*

$$e_{d+1} = -\sum_{i=1}^{d} e_i.$$

We introduce the convention that $z^{d+1} = 0$. We associate to x the ordered partition $\omega = (\omega_1, \ldots, \omega_{l+1})$ of $[d+1]$ where the ω_i are obtained by sorting the z^i in decreasing order. Specifically, with $\omega_i = \{\omega_i(1), \ldots, \omega_i(m_i)\}$, we have (see Figure 2):

$$1 > z^{\omega_1(1)} = \cdots = z^{\omega_1(m_1)} > \cdots > z^{\omega_l(1)} = \cdots = z^{\omega_l(m_l)}$$

$$> z^{\omega_{l+1}(1)} = \cdots = z^{\omega_{l+1}(m_{l+1})} = 0. \tag{1}$$
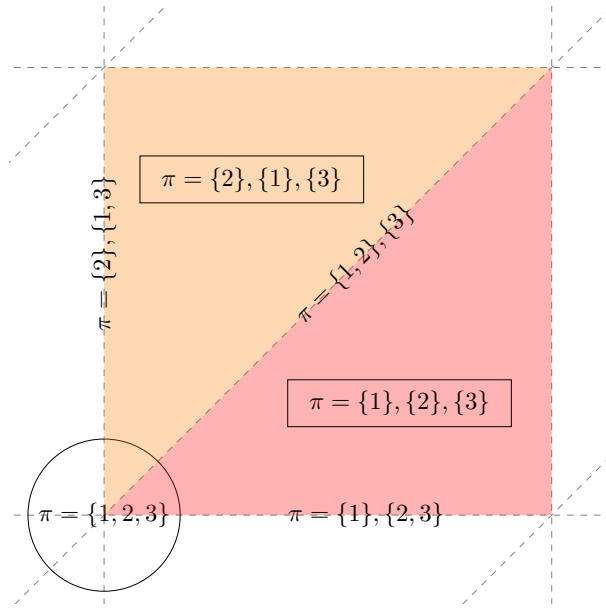
Figure 2 The ordered partitions associated to the faces of the FK-triangulation of $\mathbb{R}^2$ that have the same minimal vertex v_0 (circled).

▶ **Lemma 11.** *Suppose that $\omega = (\omega_1, \ldots, \omega_{l+1})$ is an ordered partition of $[d+1]$ such that $d+1 \in \omega_{l+1}$, and let $\sigma = \{v_0, \ldots, v_l\}$ be the l-simplex whose vertices are the points*

$$v_0 = (\lfloor x^1 \rfloor, \ldots, \lfloor x^d \rfloor), \qquad v_i = v_{i-1} + \sum_{j \in \omega_i} e_j \qquad i = 1, \ldots, l. \tag{2}$$

Then x is a point in the relative interior of σ if and only if $z^i = x^i - \lfloor x^i \rfloor$, $i = 1, \ldots, d+1$ (with, as above, $z^{d+1} = 0$), satisfy (1).

Proof. Because the whole problem is translation invariant, we assume that $v_0 = 0$ without loss of generality, so that the expressions are shorter. Using barycentric coordinates, $z \in \sigma$ can be written as

$$z = \sum_{i=0}^{l} \lambda_i v_i = \sum_{i=0}^{l} \lambda_i \sum_{k=1}^{i} \sum_{j \in \omega_i} e_j$$

$$= \lambda_l \left(\sum_{k \in \omega_l} e_k \right) + (\lambda_l + \lambda_{l-1}) \left(\sum_{k \in \omega_{l-1}} e_k \right) + \cdots + (\lambda_l + \cdots + \lambda_1) \left(\sum_{k \in \omega_1} e_k \right). \tag{3}$$

Here the $\lambda_i > 0$, $i \in [0, l]$, $\sum_{i=0}^{l} \lambda_i = 1$, are the barycentric coordinates of z in σ. We have

$$\alpha_{\omega_l(1)} = \cdots = \alpha_{\omega_l(m_l)} = \lambda_l$$

$$\vdots$$

$$\alpha_{\omega_1(1)} = \cdots = \alpha_{\omega_1(m_1)} = \lambda_l + \cdots + \lambda_1 \tag{4}$$

From (3), we see that $\alpha_{\omega_i(j)}$ is the $\omega_i(j)$th coordinate of z, denoted by $z^{\omega_i(j)}$, while all coordinates $z^{\omega_{l+1}(1)}, \ldots, z^{\omega_{l+1}(m_{l+1})}$ are zero, because $e_{\omega_{l+1}(i)}$ does not occur in (3), for all i. Moreover, because $\lambda_l + \cdots + \lambda_i > \lambda_l + \cdots + \lambda_{i-1}$, we see that (1) is satisfied.

Conversely, given a point z such that its coordinates satisfy (1), we can read of its barycentric coordinates with respect to the v_i, as defined by (2), from (4). ◄

▶ **Theorem 12.** *The equivalence classes of the points of $\mathbb{R}^d$ with a same ordered partition are the simplices of a triangulation of $\mathbb{R}^d$ called the FK-triangulation (see Figure 2).*

Proof. Lemma 11 implies that:

- Any face of a simplex in the FK-triangulation also lies in the FK-triangulation.
- The intersection of two simplices in the FK-triangulation also lie in the FK-triangulation.
- For any point $x \in \mathbb{R}^d$, there is a unique simplex σ such that x lies in the relative interior of σ. Indeed, x has uniquely defined barycentric coordinates with respect to the vertices of σ, and thus is mapped to a unique point in σ.

Hence the partition we have defined is a well-defined triangulation of $\mathbb{R}^d$. ◄

▶ **Remark 13.** *We note that, by construction, v_0 in Lemma 11 is the smallest vertex of σ in the lexicographical order. Lemma 11 also implies an observation of Freudenthal [18]: all d-simplices in the FK-triangulation can be described by monotone paths along the edges of the cube from vertex $(0, \ldots, 0) + v_0$ to vertex $(1, \ldots, 1) + v_0$. Conversely, any monotone path along the edges of the cubes from $(0, \ldots, 0) + v_0$ to $(1, \ldots, 1) + v_0$ gives a simplex in the FK-triangulation.*

2.3 CFK-triangulations

Freudenthal-Kuhn triangulations are closely related to Coxeter triangulations of type $\tilde{A}_d$ [11] and both are arrangements of hyperplanes as demonstrated now.

Let E be a finite set of vectors of $\mathbb{R}^d$, and consider the set of hyperplanes $H_E = \{x \in \mathbb{R}^d \mid \langle x, u \rangle = k, u \in E, k \in \mathbb{Z}\}$. In generalization of the theory of Coxeter triangulations, we call the set E the set of roots for historic reasons, as mentioned below.

These hyperplanes partition $\mathbb{R}^d$ in a cell complex called the *arrangement* of the hyperplanes. We denote it by $\mathcal{H}_E$.

▶ **Lemma 14.** *The Freudenthal-Kuhn triangulation is the hyperplane arrangement $\mathcal{H}_{E_{FK}}$ associated to the set of vectors $E_{FK} = \{e_1, \ldots, e_d\} \cup \{u_{i,j} = e_j - e_i \mid 1 \leq i < j \leq d\}$.*

Proof. Thanks to Lemma 11, we know that if $x \in \sigma$, where σ is a simplex of dimension less than d, there is at least one equality in (1) on top of $z^{d+1} = 0$. That is $x^i - \tilde{v}_0^i = x^j - \tilde{v}_0^j$ or $x^i - \tilde{v}_0^i = 0$ for some $i, j \neq d + 1$. Note that $\tilde{v}_0^i, \tilde{v}_0^j \in \mathbb{Z}$. The converse direction of Lemma 11 gives that if $x^i - \tilde{v}_0^i = x^j - \tilde{v}_0^j$ or $x^i - \tilde{v}_0^i = 0$ for some $i, j \neq d + 1$ for $x \in \mathbb{R}^d$, then there is a simplex σ of dimension strictly less than d in the FK-triangulation such that $x \in \sigma$. ◄

Observe that the norms of the vectors in E_{FK} are either 1 or $\sqrt{2}$. By definition, this implies that the distance between the two hyperplanes $\langle x, u \rangle = k$, and $\langle x, u \rangle = k + 1$, where $u \in E_{FK}$, is either 1 or $1/\sqrt{2}$.

Let H be the hyperplane of $\mathbb{R}^{d+1}$ of equation $\langle x, \mathbf{1} \rangle = 0$ where $\mathbf{1}$ is the vector of $\mathbb{R}^{d+1}$ whose coordinates are all 1. We now define a linear map μ from $\mathbb{R}^d$ to H by showing how it acts on the basis of $\mathbb{R}^d$: $\mu(e_i) = r_{1,i} = \sum_{j=1}^{i} s_j$, where $s_i = e_i - e_{i+1}$, $i = 1, ..., d$. The vectors s_j are called simple roots and play an important role in algebra. We refer to [11] for more information.

▶ **Lemma 15.** *μ maps E_{FK} bijectively onto the set E_C defined as*

$$E_C = \left\{ r_{i,j} = \sum_{l=i}^{j} s_l = e_i - e_{j+1} \,\middle|\, 1 \le i \le j \le d \right\}$$

Proof. The vector $\mu(e_i) = r_{1,i}$ lies in E_C, by definition. For $u_{i,j} \in E_{FK}$, with $i < j$, we see that

$$\mu(u_{i,j}) = \mu(e_j - e_i) = \mu(e_j) - \mu(e_i) = r_{1,j} - r_{1,i}$$

$$= \sum_{l=1}^{j} s_l - \sum_{l=1}^{i} s_l = \sum_{l=i+1}^{j} s_l = r_{i+1,j}.$$

Hence $\mu(u_{i,j})$ lies in E_C. By reading the previous calculation backwards, we see that μ^{-1} maps each $r \in E_C$ to a vector in E_{FK}. ◀

Observe that all vectors in E_C have length $\sqrt{2}$. By definition, this implies that the distance between the two hyperplanes $\langle x, u \rangle = k$, and $\langle x, u \rangle = k + 1$, where $u \in E_C$, is $1/\sqrt{2}$.

The image by μ of the Freudenthal-Kuhn triangulation is a triangulation of $\mathbb{R}^d$ which is the arrangement $\mathcal{H}_{E_C}$ associated to the set of vectors E_C. This triangulation is called the *Coxeter triangulation* of type $\tilde{A}_d$ of $\mathbb{R}^d$. By definition, it has the same combinatorial structure as the FK-triangulation. In addition, it has remarkable geometric properties [15, 11]. First, it is a non-degenerate Delaunay triangulation, and its dual complex is a Voronoi diagram. Moreover, its simplices have an exceptionally large thickness (the ratio of the smallest altitude of a simplex over its diameter or longest edge length).

We will call any triangulation of $\mathbb{R}^d$ that is the image of a Freudenthal-Kuhn triangulation under a non-degenerate affine map a Coxeter-Freudenthal-Kuhn triangulation, or CFK-triangulation for short. This includes the Coxeter triangulation of type $\tilde{A}_d$ (as embedded in $\mathbb{R}^d$).

3 Data Structure

We introduce our data structure in this section. We first consider the case of FK-triangulations in Sections 3.1 and 3.2. The extension to CFK-triangulations in Section 3.3 is straightforward, since all these triangulations have the same combinatorial structure.

3.1 Permutahedral representation of FK-triangulations

Cycles and the permutahedron. In Remark 13 we have seen that simplices can be described by monotone paths (increasing coordinates) along the the edges of the cube. As
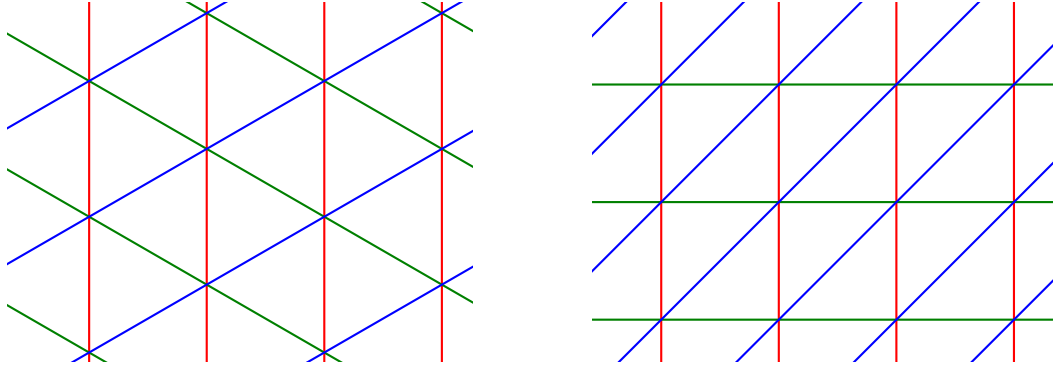
■ **Figure 3** The Coxeter and Freudenthal-Kuhn triangulations in the plane.

observed by Eaves [16], these monotone paths can be made into a cycle using the extra vector $e_{d+1} = -\sum_{i=1}^{d} e_i$ because by construction

$$v_0 = v_l + \sum_{i \in \omega_{l+1}} e_i,$$

with ω as in Definition 10. Because it is a cycle, we can take any vertex of the cycle as a starting point, which means that v_0 no longer has a special role as a starting point of a monotone edge walk. A cycle can now be represented by an ordered partition of $[d+1]$, for which it is not longer necessary that $d+1$ lies in ω_{l+1}, and an (arbitrary) starting point. We now formalize these general cyclical paths:

▶ **Definition 16** (Permutahedral representation). *Let* $(v_0, \omega) \in \mathbb{Z}^d \times OP_{l+1}[d]$. *To this pair we associate a simplex* $\sigma^\omega = \{v_0 = v_0^\omega, v_1^\omega, \ldots, v_l^\omega\}$ *with*

$$v_i^\omega = v_{i-1}^\omega + \sum_{i \in \omega_i} e_i \qquad\qquad i = 1, \ldots, l. \tag{5}$$

We say that (v_0, ω) *is the permutahedral representation of the simplex* σ^ω. *If* $d+1 \in \omega_{l+1}$, *we say that* (v_0, ω) *is the* canonical permutahedral representation *of* σ^ω. *In this case,* σ^ω *is a simplex in the FK-triangulation in the cube of which* v_0 *is the minimal vertex with respect to the lexicographical order, as we have seen above.*

In Lemma 19, and Proposition 20, we will see that, more generally, $\{(v_0, \omega) \mid \omega \in OP[d+1]\}$ is the star of v_0 in the FK-triangulation, where we identify simplices with their permutahedral representations.

▶ **Definition 17** (Cyclic shifts). *Let* (v_0, ω) *be a permutahedral representation. We define the cyclic shift of* (v_0, ω) *of length* k *to the left as* (v_0', ω'), *where*

$$v_0' = v_0 + \sum_{j=1}^{k} \sum_{i \in \omega_j} e_i \qquad\qquad \omega_j' = \omega_{(j+k-1) \bmod (l+1)+1}. \tag{6}$$

Here we use the convention that the sum from 1 to 0 is empty. We write $(v_0', \omega') = (v_0, \omega) \oplus k$.

▶ **Lemma 18.** *The cyclic shift* $(v_0', \omega') = (v_0, \omega) \oplus k$ *defines the same simplex as* (v_0, ω).

Proof. Follows by inserting (6) in (5). ◀
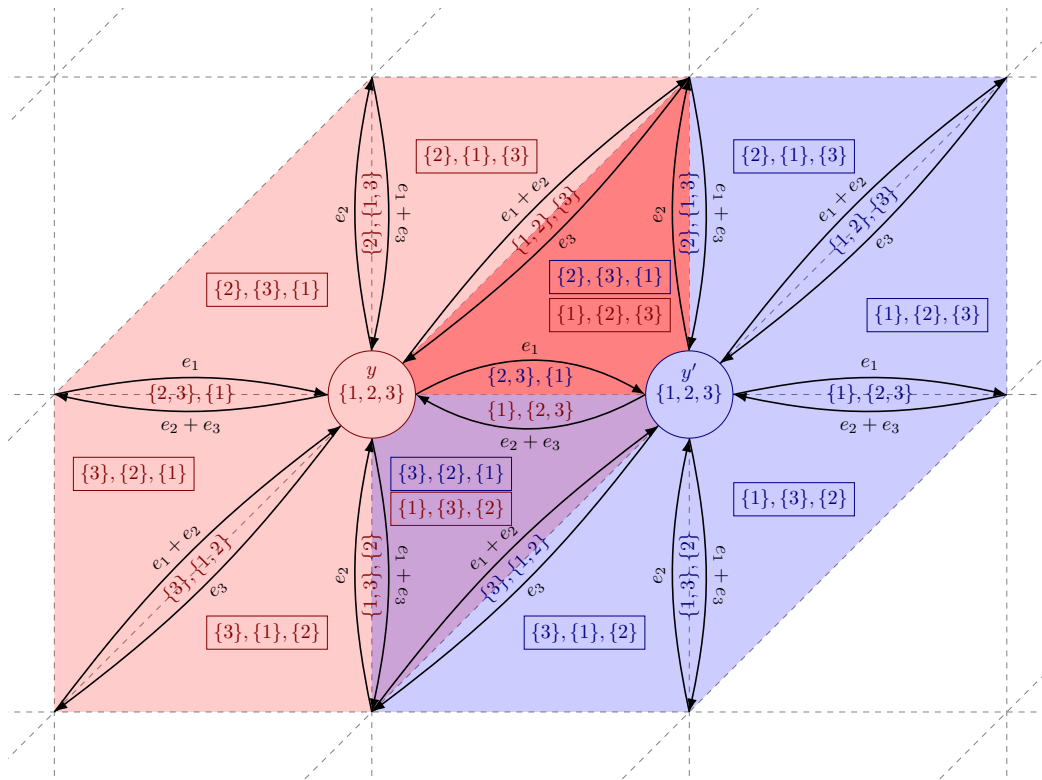
■ **Figure 4** The permutahedral representation of the simplices in the stars of vertices y and y'.

We now prove that the all permutahedral representations for a fixed v_0, form the star of v_0. This is a crucial property that will be used to efficiently compute faces, and cofaces, and traverse the triangulation.

▶ **Lemma 19.** *The set $\{(v_0, \omega) \mid \omega \in OP[d+1]\}$, where $OP[d+1]$ is the set of all ordered partitions of $[d+1]$, gives all the simplices in the star of v_0 in FK-triangulation.*

Proof. Let (v_0, ω), with $\omega \in OP_{l+1}[d+1]$, be such that $d+1 \in \omega_k$. Let $(v'_0, \omega') = (v_0, \omega) \oplus (l-k+1)$. By Definition 17, and Lemma 18, (v_0, ω), and (v'_0, ω') represent the same simplex. Moreover $d+1 \in \omega'_{l+1}$, that is (v'_0, ω') is a canonical permutahedral representation. This implies that (v'_0, ω') lies in the FK-triangulation by Lemma 11, and Theorem 12.

Conversely, suppose that (v'_0, ω') is the canonical permutahedral representation of a simplex in the star of v_0, that is there is some k such that $v'_k = v_0$, with v'_k as in (2). Then $(v_0, \omega) = (v'_0, \omega') \oplus k$ is also a permutahedral representation of the same simplex. ◀

Faces. From (5) it is clear that merging two consecutive parts in the ordered partition $\omega = (\omega_1, \ldots, \omega_{l+1})$ corresponds to removing a vertex from the simplex, that is taking a facet. Here we stress that we allow to merge ω_1, and ω_{l+1}, but in that case we have to change the base point of the cycle to $v_0 + \sum_{l \in \omega_1} e_l$ to obtain the canonical representation. For example, when looking at the two dimensional example in Figure 4, we see that the edges that contain y in the red triangle with permutahedral representation $(y, (\{1\}, \{2\}, \{3\}))$ are $(y, (\{1,2\}, \{3\}))$, and $(y, (\{1\}, \{2,3\}))$. The third edge of the red triangle is $(y', (\{2\}, \{1,3\}))$.

Generally, given an ordered partition ω in $l+1$ parts all $(l-j)$-faces can be found by merging j consecutive parts in ω (for example merging ω_1 with ω_2, and ω_3 with ω_4), where we allow ω_{l+1} to merge with ω_1, but in this case we again need to change the base point to obtain the canonical representation.

Because the combinatorial structure of the faces is compatible with the permutahedron, Lemma 19 immediately gives the following result. We recall that two complexes are dual if there is a bijection between the faces that inverses the inclusion relationships (see for example [8, Section 11.3]).

▶ **Proposition 20.** *The star of v_0 is dual to a permutahedron (combinatorially).*

This proposition explains the nomenclature permutahedral representation.

This is equivalent to the following more geometric result:

▶ **Proposition 21.** *The Voronoi cell of a Coxeter triangulation of type $\tilde{A}_d$ is a permutahedron.*

This can be found in [13, Chapter 21, Section 3.F], see also [12]. We note that Coxeter triangulations of type $\tilde{A}_d$ are combinatorially equivalent to FK-triangulations as discussed below in Section 2.3. In the appendix we give a new proof that is more direct than the one in [13].

Duality. We can associate to a FK-triangulation $\mathcal{T}$ its dual complex $\mathcal{T}^*$. Since $\mathcal{T}$ is a simplicial complex, $\mathcal{T}^*$ is a simple complex, that is a cell complex whose faces are all simple polytopes [8]. By Proposition 20, each d-dimensional cell of $\mathcal{T}^*$ is a d-permutahedron.

3.2   Basic operations on FK-triangulations

Point location. Given a point $x \in \mathbb{R}^d$ Lemma 11 tells us how to find the canonical permutahedral representation of the simplex in which x is contained. The complexity of point location is dominated by the sorting of the $z^i = x^i - \lfloor x^i \rfloor$, which takes $O(d \log d)$ time, and requires $O(d)$ space.

Face computation. Let σ be an l-simplex whose canonical permutahedral representation is (v_0, ω), where ω is an ordered partition of $[d+1]$ into $l+1$ parts. The computation of all k-faces of σ goes as follows. We use Ehrlich's subset generation algorithm [17] to compute all the subsets of $k+1$ elements from $\{v_0, \ldots, v_l\}$. Let $\tau = \{v_{m_0}, \ldots, v_{m_k}\}$ be such a subset. τ is a k-face of σ. We then compute the canonical permutahedral representation of all those k-faces τ.

We first sort the m_i so that $m_0 < \cdots < m_k$ using counting sort. Then, the canonical permutahedral representation $(\tilde{v}_0', \omega')$ of τ is found by merging consecutive parts of ω so as to obtain $k+1$ parts as follows :

$$v_0' = v_{m_0} = v_0 + \sum_{j \in \omega_1} e_j + \ldots + \sum_{j \in \omega_{m_0-1}} e_j$$

$$\omega_i' = \omega_{m_{i-1}} \cup \ldots \cup \omega_{m_i-1} \quad \text{for } i \in \{1, \ldots, k\}$$

$$\omega_{k+1}' = (\omega_1 \cup \ldots \cup \omega_{m_0-1}) \cup (\omega_{m_k} \cup \ldots \cup \omega_{l+1}).$$

The complexity of computing all subsets of $k+1$ vertices of σ using Ehrlich's algorithm takes time $O(k+s)$ where $s = \binom{l+1}{k+1}$ is the number of subsets. Computing, for each such k-simplex its permutahedral representation takes $O(d)$ time.

▶ **Lemma 22.** *Let σ be an l-simplex in the FK-triangulation of $\mathbb{R}^d$ given by its canonical permutahedral representation. Computing the canonical permutahedral representations of*

all its k-faces can be done in time $O(ds)$, where $s = \binom{l+1}{k+1}$ is the number of k-faces of an l simplex. The space complexity of the algorithm is $O(l)$.

Coface computation. Computing the faces of a simplex σ consists in coarsifying its ordered partition. The computation of cofaces is the reverse. Here we refine the ordered partition. Specifically, if σ is a k-simplex represented by its canonical permutahedral representation (v_0, ω), and we want to compute its l-cofaces, we need to compute all refinements of ω into $l + 1$ parts.

More precisely, we need to subdivide each ω_i in $a_i \le |\omega_i|$ subparts so that $\sum_{i=1}^{k+1} a_i = l+1$. This can be done in time proportional to the number $k + 1$ of the generated subparts. We then need to consider all the permutations of these subparts since we are interested in ordered partitions. Using known algorithms by Walsh [26], and Ruskey and Savage [24], we can compute all the ordered partitions associated to the l-cofaces of σ in time proportional to the number of such cofaces. We thus obtain all the permutahedral representations (v_0, ω') of all the l-cofaces of σ.

It is important to notice that all cofaces of σ have v_0 as a vertex. However v_0 is not necessarily the minimal vertex of some of the computed cofaces. We thus have to identify the minimal vertex of each computed coface, and use cyclic shifts (as in Lemma 19) to obtain the canonical permutahedral representation of the coface. The next Lemma follows. The bound on the number s of cofaces follows, by duality, from Corollary 9.

▶ **Lemma 23.** *Let σ be a k-simplex in the FK-triangulation of $\mathbb{R}^d$ given by its permutahedral representation. Computing the permutahedral representations of all its l-cofaces can be done in time $O(ds)$, where*

$$s = p_{d-l, d-k} \le \frac{1}{2^{\min(l, d-l)}} \binom{d-k}{d-l} (d-k+1)!$$

is the number of l-cofaces of a k-simplex in the FK-triangulation. The space complexity of the algorithm is $O(d)$.

3.3　Data structure for CFK-triangulations

We store a CFK-triangulation as follows. The combinatorial structure of the triangulation is given through the canonical permutahedral representation of its simplices, and the algorithms from Section 2.2. The geometry of the triangulation is specified by the affine transformation that maps the FK-triangulation of $\mathbb{R}^d$ to the CFK-triangulation. The affine transformation is given by a $d \times d$ matrix Λ, and a d-vector b. For the FK-triangulation, Λ is the identity matrix, and $b = 0$; therefore no storage is required. For the Coxeter triangulation of type $\tilde{A}_d$, Λ is sparse as indicated in Section 2.3.

4　Experimental results

The data structure and the basic operations have been implemented in C++ and are currently under review to be integrated in the GUDHI library. We report on the execution time of the face and coface generation algorithms for the FK-triangulations.

In Tables 1-4, we consider an ambient space of moderate dimension $d = 30$ and compute the higher dimensional faces of various high dimensional simplices, of dimensions ranging from 22 to 30.

Each entry in Table 1 corresponds to the total time in milliseconds of computing all the k-dimensional faces of a set of l-dimensional simplices in $\mathbb{R}^{30}$. The l-dimensional simplices are picked at random in the triangulation and the results are averaged over $1\,000$ simplices. Note that the time $11\,904.7ms$ is the time of computing all $5\,852\,925$ faces of dimension 22 of a simplex of dimension 30.

Table 2 shows the same running times per computed face. As we can see, except for the case $l = k$, the running time per computed face is around $2\mu s$.

Face dimension k		22	23	24	25	26	27	28	29
	22	0.006							
	23	0.042	0.006						
	24	0.503	0.05	0.008					
Simplex dimension l	25	4.88	0.645	0.058	0.008				
	26	33.76	5.697	0.697	0.062	0.008			
	27	162.114	35.108	6.824	0.758	0.064	0.008		
	28	885.293	190.441	40.856	6.906	0.739	0.058	0.006	
	29	3420.99	973.455	246.88	49.896	6.657	0.735	0.058	0.006
	30	11904.7	4175.92	1247.97	275.776	50.932	7.348	0.778	0.058

Table 1 Total running time of the face generation algorithm (in milliseconds).

Face dimension k		22	23	24	25	26	27	28	29
	22	0.006							
	23	0.0018	0.006						
	24	0.0017	0.002	0.008					
Simplex dimension l	25	0.0019	0.002	0.0022	0.008				
	26	0.0019	0.0019	0.002	0.0023	0.008			
	27	0.0016	0.0017	0.0021	0.002	0.0023	0.006		
	28	0.0019	0.0016	0.0017	0.0019	0.0018	0.002	0.006	
	29	0.0017	0.0016	0.0017	0.0018	0.0016	0.0017	0.0019	0.006
	30	0.0015	0.0016	0.0017	0.0016	0.0016	0.0016	0.0017	0.0019

Table 2 Running time of the *face* generation algorithm *per computed face* (in milliseconds).

In Tables 3 and 4, we present analogous tables for the coface computation algorithm. Similarly, the running time per computed coface in Table 4 is around $2\mu s$ with the exception of when k is close to l.

Coface dimension l		23	24	25	26	27	28	29	30
	22	0.11	1.274	9.577	43.848	86.699	96.407	59.935	15.487
	23	0.043	0.114	0.729	3.499	9.337	13.523	10.058	3.049
	24		0.047	0.1	0.381	1.183	2.132	1.871	0.653
Simplex dimension k	25			0.046	0.097	0.23	0.423	0.426	0.193
	26				0.047	0.076	0.128	0.15	0.093
	27					0.049	0.069	0.081	0.063
	28						0.047	0.061	0.054
	29							0.05	0.053
	30								0.05

Table 3 Total running time of the *coface* generation algorithm (in milliseconds).

Coface dimension l		23	24	25	26	27	28	29	30
	22	0.002	0.0013	0.0013	0.0015	0.0016	0.0016	0.0016	0.0017
	23	0.042	0.003	0.0017	0.0016	0.0016	0.0016	0.0016	0.0017
	24		0.045	0.004	0.0019	0.0017	0.0017	0.0017	0.0018
Simplex dimension k	25			0.045	0.0053	0.0025	0.002	0.0019	0.0022
	26				0.047	0.0073	0.0035	0.0028	0.0036
	27					0.048	0.0103	0.0058	0.0068
	28						0.048	0.0145	0.0133
	29							0.05	0.026
	30								0.05

Table 4 Running time of the *coface* generation algorithm *per computed face* (in milliseconds).

The next results are motivated by the problem of tracing a manifold of low dimension m embedded in $\mathbb{R}^d$ for high d. The crucial operations in this context consist in computing the facets and cofacets of simplices of codimension m in a triangulation of $\mathbb{R}^d$ [4].

In Table 5, we present the execution time of the *facet* generation algorithm applied to simplices of low codimension m, ranging from 1 to 7, in FK-triangulations of high dimensions d (up to $d = 400$). In Table 6, we present the execution time of the *cofacet* generation algorithm under the same circumstances.

Ambient dimension d		50	100	150	200	250	300	350	400
	1	0.166	0.612	1.438	2.862	5.376	8.69	12.184	15.924
	2	0.166	0.643	1.417	2.858	5.607	8.375	11.806	16.261
	3	0.168	0.607	1.395	2.888	5.866	8.232	12.008	16.527
Face codimension m	4	0.162	0.589	1.373	2.864	5.491	8.447	11.936	16.08
	5	0.154	0.587	1.349	2.76	5.77	8.371	11.814	15.88
	6	0.148	0.579	1.321	2.737	5.735	8.351	12.038	15.798
	7	0.136	0.575	1.313	2.553	5.701	8.313	12.11	15.754

■ **Table 5** Average running times in milliseconds of the *facet* generation algorithm.

Ambient dimension d		50	100	150	200	250	300	350	400
	1	0.068	0.134	0.228	0.281	0.423	0.605	0.611	0.848
	2	0.082	0.17	0.267	0.341	0.483	0.723	0.731	0.966
	3	0.098	0.194	0.303	0.401	0.525	0.733	0.866	1.124
Simplex codimension m	4	0.112	0.226	0.351	0.467	0.665	0.806	0.974	1.295
	5	0.132	0.265	0.423	0.545	0.966	0.928	1.128	1.477
	6	0.162	0.329	0.515	0.713	0.948	1.124	1.361	1.76
	7	0.2	0.415	0.651	0.878	1.166	1.421	1.784	2.283

■ **Table 6** Average running times in milliseconds of the *cofacet* generation algorithm.

A graphical display of the results of Tables 5 and 6 is shown in Figure 5.
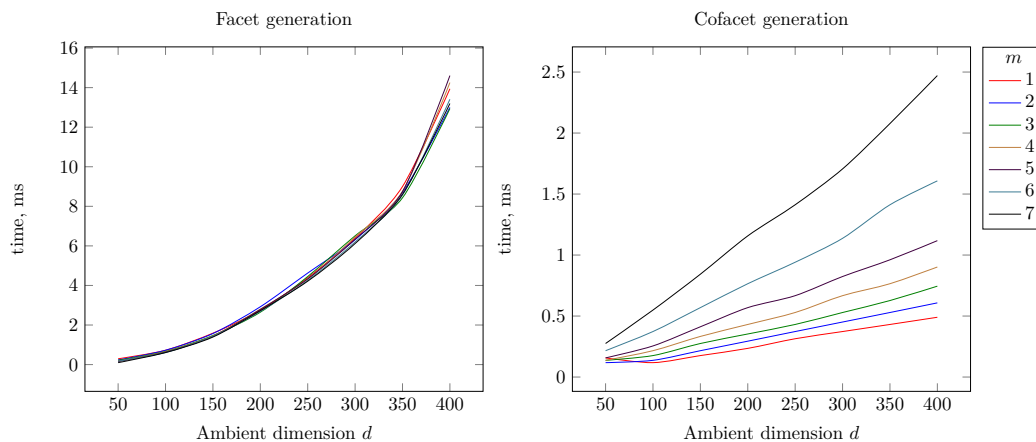
■ **Figure 5** Graphical display of the results of Tables 5 and 6.

5 Conclusion

We have introduced a data structure to represent any triangulation in a family of highly regular triangulations of $\mathbb{R}^d$, which we called the CFK-triangulations. This family includes the celebrated Freudenthal-Kuhn triangulation and Coxeter triangulations of type $\tilde{A}_d$. The representation is implicit and extremely compact, which makes the usage of these triangulations almost as easy and efficient as that of Cartesian grids. This is advantageous in high dimensions, because a cube has 2^d vertices while a simplex has only $d + 1$ vertices. We refer to our companion paper [5], where we describe how this data structure can be used to trace isomanifolds of $\mathbb{R}^d$ of any intrinsic dimension, in time that is polynomial in the ambient dimension.

In this paper, we have only considered uniform triangulations where each simplex has (almost) the same diameter. A natural and rather easy extension of the present work would be to generalize the data structure so as to provide different resolutions in different regions.

References

1   Eugene Allgower and Kurt Georg. *Numerical continuation methods: an introduction*, volume 13. Springer Science & Business Media, 1990.

2   M. A. Armstrong. *Groups and Symmetry*. Springer, 1988.

3   Dominique Attali, André Lieutier, and David Salinas. Efficient data structure for representing and simplifying simplicial complexes in high dimensions. *International Journal of Computational Geometry & Applications*, 22(04):279–303, 2012.

4   Jean-Daniel Boissonnat, Siargey Kachanovich, and Mathijs Wintraecken. A compact data structure for high dimensional Coxeter-Freudenthal-Kuhn triangulations. Submitted to the International Symposium on Computational Geometry (SoCG2021), 2020.

5   Jean-Daniel Boissonnat, Siargey Kachanovich, and Mathijs Wintraecken. Tracing isomanifolds in $\mathbb{R}^d$ in time polynomial in d. Submitted to the International Symposium on Computational Geometry (SoCG2021), 2020.

6   Jean-Daniel Boissonnat, CS Karthik, and Sébastien Tavenas. Building efficient and compact data structures for simplicial complexes. *Algorithmica*, 79(2):530–567, 2017.

7   Jean-Daniel Boissonnat and Clément Maria. The simplex tree: An efficient data structure for general simplicial complexes. *Algorithmica*, 70(3):406–427, 2014. URL: https://doi.org/10.1007/s00453-014-9887-3, doi:10.1007/s00453-014-9887-3.

8   Jean-Daniel Boissonnat and Mariette Yvinec. *Algorithmic Geometry*. Cambridge Texts in Applied Mathematics. Cambridge University Press, 1998.

9   Nicolas Bourbaki. Lie groups and Lie algebras. Chapters 4–6. Translated from the 1968 French original by Andrew Pressley. Elements of Mathematics, 2002.

10   Yen-Chi Chen. Solution manifold and its statistical applications, 2020. arXiv:2002.05297. arXiv:2002.05297.

11   Aruni Choudhary, Siargey Kachanovich, and Mathijs Wintraecken. Coxeter triangulations have good quality. *Mathematics in Computer Science*, 14:141–176, 2020. URL: https://doi.org/10.1007/s11786-020-00461-5.

12   Aruni Choudhary, Michael Kerber, and Sharath Raghvendra. Polynomial-sized topological approximations using the permutahedron. In Sándor P. Fekete and Anna Lubiw, editors, *32nd International Symposium on Computational Geometry, SoCG 2016, June 14-18, 2016, Boston, MA, USA*, volume 51 of *LIPIcs*, pages 31:1–31:16. Schloss Dagstuhl - Leibniz-Zentrum für Informatik, 2016. URL: https://doi.org/10.4230/LIPIcs.SoCG.2016.31, doi:10.4230/LIPIcs.SoCG.2016.31.

13   J. H. Conway and N. J. A. Sloane. *Sphere-packings, Lattices, and Groups*. Springer-Verlag New York, Inc., New York, NY, USA, 1987.

14 Harold S. M. Coxeter. Discrete groups generated by reflections. *Annals of Mathematics*, pages 588–621, 1934.

15 David P. Dobkin, Allan R. Wilks, Silvio V. F. Levy, and William P. Thurston. Contour tracing by piecewise linear approximations. *ACM Transactions on Graphics (TOG)*, 9(4):389–423, 1990.

16 B. Curtis Eaves. *A course in triangulations for solving equations with deformations*, volume 234. Lecture Notes in Economics and Mathematical Systems, 1984.

17 Gideon Ehrlich. Loopless algorithms for generating permutations, combinations, and other combinatorial configurations. *Journal of the ACM (JACM)*, 20(3):500–513, 1973.

18 Hans Freudenthal. Simplizialzerlegungen von beschrankter flachheit. *Annals of Mathematics*, pages 580–582, 1942.

19 James E. Humphreys. *Reflection groups and Coxeter groups*, volume 29. Cambridge university press, 1992.

20 M. Maes and B. Kappen. On the permutahedron and the quadratic placement problem. *Philips Journal of Research*, 46(6):267–292, 1992.

21 Chohong Min. Simplicial isosurfacing in arbitrary dimension and codimension. *Journal of Computational Physics*, 190(1):295–310, 2003.

22 Timothy S. Newman and Hong Yi. A survey of the marching cubes algorithm. *Computers & Graphics*, 30(5):854 – 879, 2006. URL: `http://www.sciencedirect.com/science/article/pii/S0097849306001336`, `doi:https://doi.org/10.1016/j.cag.2006.07.021`.

23 B.C. Rennie and A.J. Dobson. On Stirling numbers of the second kind. *Journal of Combinatorial Theory*, 7(2):116 – 121, 1969. URL: `http://www.sciencedirect.com/science/article/pii/S0021980069800451`, `doi:https://doi.org/10.1016/S0021-9800(69)80045-1`.

24 Frank Ruskey and Carla D. Savage. Gray codes for set partitions and restricted growth tails. *Australasian J. Combinatorics*, 10:85–96, 1994.

25 Michael J. Todd. *The computation of fixed points and applications*, volume 124. Lecture Notes in Economics and Mathematical Systems, 1976.

26 Timothy R. Walsh. Loop-free sequencing of bounded integer compositions. *Journal of Combinatorial Mathematics and Combinatorial Computing*, 33:323–345, 2000.

27 G. M. Ziegler. *Lectures on Polytopes*. Graduate Texts in Mathematics. Springer New York, 2012. URL: `https://books.google.fr/books?id=xd25TXSSUcgC`.

A   Proof

Proof of Proposition 21. We start by recalling a number of results. Let $P = \{(x^i) \in \mathbb{R}^{d+1} \mid \sum_i x^i = 0\}$ and consider the d-simplex with vertices u_k in P.

$$u_0 = \left(0^{\{d+1\}}\right) \qquad u_k = \left(\left(-\frac{d+1-k}{d+1}\right)^{\{k\}}, \left(\frac{k}{d+1}\right)^{\{d+1-k\}}\right), \qquad k \in [d],$$

where $x^{\{k\}}$ denotes k consecutive coordinates x. This simplex is a simplex in the Coxeter triangulation, as defined in Section 2.3. In [11] we have seen that the circumcentre of this simplex is

$$c = \left(-\frac{d-2i}{2(d+1)}\right),$$

with $i \in \{0, \ldots, d\}$. The circumcentre of a Delaunay simplex is a Voronoi vertex. We recall that

- All simplices in the star of 0 in the Coxeter triangulation are found by consecutive reflection of a single simplex (in this star) in the hyperplanes of $\mathcal{H}_{E_C}$ that go through 0, that is the hyperplanes with normals $r_{j,k} = e_j - e_k$, with $j \neq k$. See for example [9, 19, 11]. We also call these reflections the action of the Weyl group.

578 ▪ The reflection $R_{j,k}$ in a plane that goes through the origin with normal $r_{j,k}$ is given by

579
$$R_{j,k}(v) = v - 2\frac{v \cdot r_{j,k}}{r_{j,k} \cdot r_{j,k}} r_{j,k} = v - (v \cdot r_{j,k})r_{j,k}.$$

580 We find that

581
$$R_{j,k}(c)^i = (c - (c \cdot r_{j,k})r_{j,k})^i = -\frac{d - 2i}{2(d+1)} - \frac{2j - 2k}{2(d+1)}(\delta_{ij} - \delta_{ik}),$$

582 which permutes the jth and kth coordinate of c. Here we used the upper index i to denote
583 the ith coordinate. Using the cycle notation for the permutation group, see for example [2,
584 Chapter 6], this coincides the 2-cycle $(j\,k)$. Let now

585
$$c_\pi = \left(-\frac{d - 2\pi_i}{2(d+1)}\right),$$

586 with $\{\pi_i\}$ some permutation of $\{0, \ldots, d\}$. We find that

587
$$R_{j,k}(c_\pi)^i = (c_\pi - (c_\pi \cdot r_{j,k})r_{j,k})^i = -\frac{d - 2\pi_i}{2(d+1)} - \frac{2\pi_j - 2\pi_k}{2(d+1)}(\delta_{ij} - \delta_{ik}),$$

588 which again permutes the jth and kth coordinate. Now recall that all permutations are
589 generated by 2-cycles, see for example [2, Theorem 6.1]. This implies that, for any permutation
590 π, we can find c_π from c by the action of the Weyl group. This also means that we have
591 explicitly described the Voronoi cell of 0 in the Coxeter triangulation of type $\tilde{A}_d$ as a
592 permutahedron. Because of symmetry, this now holds for any Voronoi cell. ◀